Forschungszentrum Karlsruhe
in der Helmholtz-Gemeinschaft

Wissenschaftliche Berichte

FZKA 6668

Elements of a fracture mechanics concept for the cleavage fracture behaviour of RAFM steels using local fracture criteria

Final Report for
Task TW1-TTMS-005/D3

H. Riesch-Oppermann, E. Diegele

Institut für Materialforschung
Programm Kernfusion
Association Forschungszentrum Karlsruhe / EURATOM

Forschungszentrum Karlsruhe GmbH, Karlsruhe

2002

Impressum der Print-Ausgabe:

Als Manuskript gedruckt

Forschungszentrum Karlsruhe GmbH
Postfach 3640, 76021 Karlsruhe

Mitglied der Hermann von Helmholtz-Gemeinschaft
Deutscher Forschungszentren (HGF)

ISSN 0947-8620

Abstract

An effort is made within the European Fusion Technology Programme framework to obtain a fracture mechanics description of the material behaviour in the ductile to brittle transition-regime using local fracture criteria. This report summarizes the necessary procedural steps towards the development of an according design code scheme. It makes heavy use of available code schemes such as the British Energy R6-Code or the ESIS P6 procedure and specializes in application to the class of low activation materials that are envisaged for ITER.

Through an integrated approach using a numerical stress analysis at experimentally observed fracture loads of notched tensile specimens, a statistical evaluation of cleavage fracture parameters can be performed. The report contains a description of the necessary steps for the experimental characterization and the numerical analysis as well as results for the two RAFM steel variants F82Hmod and EUROFER 97 which serve as basis for the verification of the method. Statistical inference methods are addressed as well as fractographic investigations that are essential for the verification of the approach via numerical prediction of the fracture origin distribution. Limits of the current methodology are given and topics of future research are indicated.

Zusammenfassung

Grundbegriffe einer bruchmechanischen Beschreibung des Sprödbruchverhaltens für niedrigaktivierbare Stähle auf Basis lokaler Versagenskriterien

Innerhalb des Europäischen Fusionsprogramms wird eine bruchmechanische Beschreibung des Materialverhaltens im Bereich des spröd-duktilen Übergangs auf Basis lokaler Versagenskriterien angestrebt. In diesem Bericht werden die dazu notwendigen Schritte für die Entwicklung eines entsprechenden Designcodes zusammengefaßt. Der Bericht greift auf bereits vorhandene Vorschriften wie den R6-Code von British Energy oder die ESIS P6 Prozedur zurück und fokussiert auf deren Anwendbarkeit für die zum Bau von ITER als Strukturmaterialien anvisierten ferritisch-martensitischen Stähle mit niedriger Aktivierbarkeit.

Mittels eines einheitlichen Ansatzes einer numerische Spannungsanalyse für experimentell ermittelte Lastniveaus beim Bruch gekerbter Rundzugproben kann eine statistische Charakterisierung der Sprödbruchparameter erfolgen. Der vorliegende Bericht enthält eine Zusammenstellung der notwendigen Schritte für die experimentelle Charakterisierung und die numerische Analyse sowie Ergebnisse für die beiden Stahlsorten F82Hmod und EUROFER 97, die gleichzeitig als Basis zur Beurteilung der methodischen Vorgehensweise dienen. Es wird auf Methoden der schließenden Statistik sowie auf fraktografische Untersuchungen eingegangen. Die Grenzen der Methodik werden aufgezeigt und Bereiche zukünftiger Untersuchungen aufgezeigt.

Contents

List of Figures

List of Tables

1 General

The present analysis is part of the **EURATOM Fusion Technology - Blanket** programme for 1999 to 2002 under EFDA Reference TW1-TTMS-005 **RAFM STEELS: Rules for Design, Fabrication, and Inspection**.

1.1 Introduction

1.1.1 Purpose

Within this framework, it is intended to apply a fracture mechanics concept for the description of the ductile-to-brittle-transition behaviour of ferritic-martensitic steels in the lower-shelf regime and to incorporate the concept into structural design coding schemes. Due to the need of transferability, a concept based on the mechanisms of ductile or brittle fracture is used for the assessment of size and geometry effects. Perspectives of future applications are cases where irradiation effects, complex mechanical as well as thermal loading conditions are to be taken into account.

In contrast to the global approaches, where geometrical limits on validity of test results are imposed to ensure transferability of test data to component design, a local approach relies on the combination of local (i.e. micro-structurally based) fracture criteria and stress field analyses of selected geometries to ensure the transferability of material data. Within a local approach transferability is thus inherently guaranteed as long as the local fracture mechanism remains unchanged. This has to be verified by suitable investigations of the fractured specimens.

A key issue of the local fracture description is the determination of the fracture parameters, which requires considerable (numerical and experimental) efforts. Fracture parameters are obtained by numerical Finite Element (FE) elasto-plastic deformation analyses of fracture tests. In the case of brittle fracture, a statistical approach is necessary because of the inherent scatter.

1.1.2 Organisation of the report

The present report contains evaluation rules for local fracture criteria together with experimental results on F82Hmod and EUROFER 97 steels. Contents are organized as follows:

Section 1.2 contains some basic information about background and application of local approach methods.

Section 1.3 addresses criteria levels used for brittle and ductile fracture, respectively.

Definitions of relevant quantities are given in Section 1.4.

The main parts of the report deal with evaluation rules for FE stress analysis 2.2, Weibull stress calculation 2.3 and fractography 2.4, describe statistical inference procedures used for parameter evaluation 3, and indicate limits of applicability 4.

Appendix B contains the necessary tables.

1.1.3 Related documents

Evaluation of cleavage fracture parameters is currently under standardization efforts in different contexts (SINTAP [24], R6 [6], ESIS [12], ASTM [10]). Part of the procedures described in this document were tested and verified within an ESIS round robin [26].

The report is intended to be essentially self-contained, however, references to R6 code [6] and ESIS P6 document [12] are made if appropriate.

1.2 Background

Body-centered cubic materials exhibit a transition from brittle (low toughness, cleavage) fracture behaviour at low temperature to ductile (microvoid initiation and coalescence) fracture at high temperature. In the transition regime, the material is characterized by a large scatter of toughness [7] and the presence of a pronounced size effect of critical toughness parameters such as K_{Ic} or J_c [20]. This behaviour can be described using ideas known as “Local Approach” [4].

1.2.1 Physical description of fracture processes

The basic background of this methodology is that global failure of the material is triggered by the local behaviour in the vicinity of stress concentrations [31]. In the cleavage regime, fracture is caused by unstable growth of crack initiation sites whose activation is thought to coincide with the onset of plastic deformation [35]. The worst (in some sense) initiation site is determining failure, which leads to an extreme value distribution of the fracture (toughness) parameter. Basic assumptions which are essential for the validity of the model are that the possible initiation sites are statistically independent and (for fracture mechanics specimens) that the stress field obeys small scale yielding (SSY) conditions. Also, it is essential that the fracture mode is purely cleavage and that there is no void initiation (i.e. no ductile damage). If these basic assumptions are violated, modification of the model is necessary to take into account the effects of gross yielding and of microvoid initiation [5].

Result of the model is the description of the dependence of toughness parameters like K_{Ic} or J_c of temperature as well as the scatter of the parameters in the different temperature regimes.

In the ductile regime, the fracture mechanism is characterized by the formation and growth of voids from inclusions. Void formation is thought to coincide with the onset of plastic deformation, the initial void volume fraction thus given by precipitations, inclusions etc.. The growth rate of voids triggered by stress triaxiality is given in the model of Rice & Tracey [25], its corrections [16] or other models, e.g. Gurson [17, 34]. Main purpose of the "Local Approach" is to combine stress and strain field analyses with micro-structural features of the material causing failure events. This approach allows predictions with respect to size effects and with respect to scatter in the material behaviour at the expense of an increased numerical effort.

Basic ideas of the Local Approach for cleavage fracture have its foundation in the long tradition of micro-mechanical investigations, theoretical as well as using fractography which all aim at a fundamental understanding of the fracture processes on a microscopic scale. Among others, there are Stroh [35] (formation of micro-cracks within grains due to inhomogeneous plastic deformation), Ritchie et al. [18, 32], Rosenfield [33], Hahn [14] etc.

Essential ingredients for a successful application of the ideas of the Local Approach consist of firstly a precise description of the initiation of unstable crack propagation and an exact description of the stress field in the material. Also an appropriate statistical treatment of the experimental data and its numerical evaluation is essential. Fractography is indispensable for an appropriate interpretation of the applied model and also to ensure that the basic assumptions of the model with respect to the fracture mode are justified.

1.2.2 Weakest link arguments

Basis of the statistical treatment of brittle fracture is the weakest link model. The basic line of arguments in the establishment of Local Approach in the field of cleavage fracture ([2, 4, 19, 22]) are based on some essential assumptions which are summarized below. The reasoning which leads to the essential relations that govern Weibull stress considerations is given in the sequel. The following assumptions characterize the micromechanical and statistical model:

- There is a large population of weak spots in the material, which can be modelled in the framework of fracture mechanics (e.g. as penny-shaped cracks)
- Failure of the material starts from and is triggered by the most dangerous 'weak spot'

- The weak spots are randomly distributed within the material
- The weak spots are acting independently, i.e. there is no interaction
- The weak spots become 'active' with the onset of plastic deformation, i.e. only weak spots within the plastic zone are relevant for failure
- The size of the weak spots is a random variable
- The critical size of a weak spot is described within the framework of fracture mechanics through a relation of the form

$$a_c(\vec{r}) = \frac{W_p}{\sigma_c^2(\vec{r})} \tag{1}$$

where W_p contains parameters of the material relevant for fracture resistance as well as crack geometry parameters and σ_c is the stress at location $\vec{r}$ that is responsible for fracture (usually the first principal stress).

Based on these assumptions, the probability for failure of a single weak spot is just the probability that its size a exceeds the critical size a_c (Eqn. 1) and is given by the relation

$$P(a > a_c) = \int_{a_c(\vec{r})}^{\infty} f_a(a)\,\mathrm{d}a \tag{2}$$

where f_a is the probability density of the size distribution of the weak spots.

Now we are prepared to calculate the probability of failure for a given specimen or component.

We will proceed in two steps. In the first step, *Step 1*, we will assume, that there is *exactly one* weak spot in the specimen. In the second step, *Step 2*, we will take into account the contribution of a random number of k weak spots per specimen.

Step 1 - One weak spot of random size in the specimen We calculate the probability Q_1 for the weak spot to cause failure of the specimen. Q_1 is given by

$$Q_1 = \frac{1}{V_{pl}} \int_{V_{pl}} \int_{a_c(\vec{r})}^{\infty} f_a(a)\,\mathrm{d}a\,\mathrm{d}V \tag{3}$$

where f_a is the probability density of the size distribution and V_{pl} denotes the volume of the plastic zone. Here, it is assumed that weak spots are distributed randomly within the plastic zone and that the location of the weak spots follows a uniform distribution. Thus, V_{pl} can be interpreted as a normalization parameter of the location distribution and $dV_{pl}\ /V_{pl}$ is the probability of having a weak spot in a randomly chosen volume dV_{pl} at an arbitrary location within the plastic zone. Now we proceed to

Step 2 - k weak spots in the specimen We now assess the probability for at least one out of a random number of k weak spots in the specimen to cause failure. If we have k independent weak spots, the survival probability R_k of the specimen is

$$R_k = (1 - Q_1)^k \tag{4}$$

where Q_1 is the failure probability of one weak spot. If there is a mean number of M weak spots per unit volume, the probability p_k of having exactly k weak spots in the plastic zone is given by the POISSON distribution with mean MV_{pl} and leads to

$$p_k = \frac{(MV_{pl})^k}{k!} \exp(-MV_{pl}) \tag{5}$$

We obtain the survival probability P_s of the specimen by summing up the contributions for all possible numbers of weak spots in the specimen

$$P_s = \sum_{k=0}^{\infty} p_k R_k \tag{6}$$

and, using Eqns. (4) and (5), we finally end up with the relation

$$P_s = \exp(-MV_{pl}Q_1) \tag{7}$$

which leads to the failure probability P_f of the following form:

$$\begin{aligned} P_f &= 1 - P_s \\ &= 1 - \exp\left(-MV_{pl}Q_1\right) \\ &= 1 - \exp\left(-M \int\limits_{V_{pl}} \int_{a_c(\vec{r})}^{\infty} f_a(a)\,\mathrm{d}a\,\mathrm{d}V \right) \end{aligned} \tag{8}$$

To determine the failure probability P_f, some knowledge of the size distribution of the weak spots is necessary. Assuming a decay of the probability density f_a which is of a power-law type: $f_a(a) \propto a^{-n}$, the second integral of Eqn. (8) takes on the following form:

$$\int_{a_c(\vec{r})}^{\infty} f_a(a)\,\mathrm{d}a = \frac{C}{n-1} a_c(\vec{r})^{-(n-1)} \tag{9}$$

with a normalization constant C. With Eqns. (1) and (9) we obtain Q_1 from Eqn. (3) as

$$Q_1 = \frac{C}{(n-1)W_p^{n-1}} \frac{1}{V_{pl}} \int\limits_{V_{pl}} \sigma_c^{2(n-1)} \, \mathrm{d}V \tag{10}$$

and it is now possible to define a new variable termed the Weibull stress σ_W. This is done by inserting Q_1 into Eqn. (8) and observing that we may write P_f in the following alternate form:

$$P_f = 1 - \exp\left(- \left(\frac{\sigma_W}{\sigma_u} \right)^m \right) \tag{11}$$

with σ_W defined through

$$\sigma_W^m = \frac{1}{V_0} \int\limits_{V_{pl}} \sigma_c^m \, \mathrm{d}V \qquad \text{with} \qquad m = 2(n-1) \tag{12}$$

and σ_u defined through

$$\sigma_u^m = \frac{(n-1)W_p^{n-1}}{MV_0C} \tag{13}$$

so that it is possible to interpret the failure probability P_f as the value of the cumulative distribution function of the Weibull stress σ_W at failure:

$$\begin{aligned} P_f &= F_{\sigma_W}(\sigma_W) \\ &= 1 - \exp\left(- \left(\frac{\sigma_W}{\sigma_u} \right)^m \right) \end{aligned} \tag{14}$$

This means, that we have introduced the Weibull stress σ_W as a random variable that characterizes the fracture resistance of the material against cleavage (brittle) fracture. The Weibull stress σ_W at fracture is a material parameter (i.e. it is independent of the stress state in the material) but may depend on temperature. (Recent work, however, indicates that this is perhaps not the case [15].) The Weibull slope m characterizes the

scatter of the Weibull stress. The C.O.V (coefficient of variation) of σ_W is a function of m alone and is given by

$$COV_{\sigma_W} = \frac{\sqrt{\Gamma(1+\frac{2}{m}) - \left(\Gamma(1+\frac{1}{m})\right)^2}}{\Gamma(1+\frac{1}{m})} \tag{15}$$

(see Fig. 1). The parameter σ_u gives the $1-1/e$ (=63.2%)-quantile of σ_W.

The unit volume V_0 which appears in eqns. (12) and (13) is introduced for dimensional purposes only and is usually set to 1mm^3. [1]

For the analysis, the Weibull stress at fracture has to be determined from suitably chosen experimental loading parameters, such as e.g. the diameter reduction for notched tensile specimens at fracture or the value of the J-integral for cracked specimens.

1.2.3 Fracture mechanics

For pre-cracked (fracture mechanics) specimens, e.g. three point bend, center cracked (CCT), compact tension (CT) or circumferentially cracked tensile specimens, a relation between the Weibull stress at fracture and the fracture toughness can be established provided that small scale yielding (SSY) prevails [23]. This relation is the basis of various so-called toughness scaling methods.

1.3 Criteria levels

1.3.1 Brittle fracture criteria

In the lower shelf regime, weakest link approach is appropriate.

1.3.2 Ductile fracture criteria

In the upper shelf regime, a ductile fracture model has to be adopted. This is not within the scope of this document.

[1] Some authors use V_0 as an additional parameter related to σ_u (see e.g. [4, 22]) chosen to be small enough that stress gradients can be neglected and large enough that the weakest link argument for finding a micro-crack of a given size still holds (e.g. 10 grains). If stress gradients are important for the fracture behaviour, this can be directly incorporated into the fracture model leading to eq. (14) at the expense of losing the meaning of σ_u and m as material parameters (see Section 4).

1.4 Definitions

Section 1.4 gives a collection of brief definitions for the usage of terms contained in this document.

1.4.1 Small scale yielding (SSY)

The plastic zone size is small compared to specimen and crack dimensions.

Small scale yielding (SSY) provides a basis for the use of LEFM in an elastic-plastic material. SSY requires the crack tip plastic zone to be much smaller than any relevant dimension of the specimen. Consequence: the stress state outside the plastic zone, but well away from the specimen boundary is characterized by the first singular term of the Williams eigen-expansion. ASTM criterion for plane-strain fracture toughness of metallic materials (E-399) [9] e.g. specifies that for CT specimens with width W, height B and crack size a the following criteria be met:

$$B,\ a,\ (W-a) >= 16* \quad \text{radius of SSY-plastic zone} \quad (= 2.5 * \frac{K^2}{\text{yield strength}^2}) \tag{16}$$

1.4.2 Triaxiality

The triaxiality ratio h is defined as

$$h = \frac{\sigma_{kk}}{3\sigma_{eq}} \tag{17}$$

where σ_{kk} is the trace of the stress tensor and σ_{eq} is the equivalent (von Mises) stress at the selected location. $\frac{\sigma_{kk}}{3}$ is the hydrostatic part of the stress tensor.

1.4.3 Average fracture strain

The average (diametral) fracture strain for axisymmetrical notched specimens is defined as:

$$\overline{\varepsilon_f} = 2\ln\left(\frac{d_0}{d_f}\right) \tag{18}$$

where d_0 and d_f are the initial diameter and the diameter at fracture, respectively, of the minimum section.

1.4.4 Average fracture stress

The average fracture stress for axisymmetrical notched specimens is defined as:

$$\overline{\sigma_f} = \frac{4F_f}{\pi d_f^2} \tag{19}$$

where d_0 and d_f are the initial diameter and the diameter at fracture, respectively, of the minimum section and F_f is the load at fracture.

1.4.5 Stress envelope

The maximum of the first principal stress is responsible for the cleavage fracture process. During loading, the first principal stress may decrease in part of the specimen/component due to stress redistribution processes. Taking the maximum for all times at each location leads to a stress envelope that gives a maximum value for the first principal stress that a specific location has seen during loading history.

1.4.6 Weibull stress

The Weibull stress σ_W is defined as

$$\sigma_W^m = \frac{1}{V_0} \int_{V_{pl}} \sigma_1^m \, \mathrm{d}V \tag{20}$$

where σ_1 is the first principal stress, m is the Weibull modulus and V_{pl} denotes the plastic zone over which the integration is carried out. The quantity V_0 is a unit volume and usually set to $1\mathrm{mm}^3$.

1.4.7 Weibull parameters

The Weibull stress σ_W is a random variate with a Weibull distribution. Its cumulative distribution function $F_{\sigma_W}(\sigma_W)$ is given by

$$F_{\sigma_W}(\sigma_W) = 1 - \exp\left(-\left(\frac{\sigma_W}{\sigma_u}\right)^m\right) \tag{21}$$

with the quantities m and σ_u as parameters of the distribution. For ferritic steels, m typically attains values of about 20, whereas the value of σ_u depends on the choice of the unit volume V_0.

1.4.8 Unit volume

The unit volume V_0 in the definition of the Weibull stress is introduced for dimensional purposes only and usually set to 1mm^3. It has to be reported because numerical values of σ_W and correspondingly of σ_u depend on the choice of V_0.

A scaling procedure allows conversion for different choices of V_0. Let V_0 and $\widetilde{V_0}$ be two differently taken reference volume values. Then, the respective values of σ_W and $\widetilde{\sigma_W}$ are given by

$$\widetilde{\sigma_W} = \left(\frac{V_0}{\widetilde{V_0}}\right)^{\frac{1}{m}} \sigma_W \tag{22}$$

with the Weibull modulus m as obtained by the maximum likelihood estimation procedure.

1.4.9 Plastic zone

The plastic zone is defined as the region within the specimen/component where the von Mises stress, σ_{eq}, exceeds the uniaxial yield stress, σ_y, of the material.

1.4.10 Maximum Likelihood estimator

The maximum likelihood procedure is used for the determination of the Weibull parameters from a Weibull stress sample. Due to the fact that the Weibull stress itself depends on one of the Weibull parameters, an iterative procedure is necessary.

1.4.11 Confidence limits

Confidence limits are used to assess the statistical uncertainty of the Weibull parameters. This is usually done according to ISO standards. (see also [12]) However, these limits are not strictly valid for iterative maximum likelihood estimation. An alternate method which does not suffer from this restriction is described in Section 3.3.

2 Evaluation rules; Procedure

Cleavage fracture parameters are obtained by numerical integration of the stress field of fractured specimens. The evaluation procedure in this section is described using results of axisymmetrically notched tensile bar specimens [12, 6].

Use of pre-cracked specimens is currently under consideration but poses additional difficulties in experimental setup as well as in numerical modelling and is therefore currently not incorporated in code schemes. A promising exception is the use of circumferentially precracked axisymmetric tensile specimens, where numerical modelling is possible using a two-dimensional analysis. Here, efforts are made during the last few years within the R6 code [6] to use this specimen geometry for cleavage fracture characterization. A draft procedure for the use of pre-cracked specimens to obtain cleavage fracture parameters is currently being under development within the European Structual Integrity Society (ESIS).

2.1 Experimental data base

Axisymmetric notched tensile specimens are used for the analysis of cleavage fracture behaviour.

2.1.1 Specimen geometry

Specimen dimensions as in Ref. [12] are based on a minimum diameter (i.e. measured across the notch root) of 10mm. If availability of material or testing equipment are limited, smaller values are possible. Care has to be taken to select a specimen length that is sufficient to avoid inference from the gripping system. (i.e. the length between shoulders exceeds 2 times specimen diameter) The minimum diameter should be selected large enough to avoid too much plastic deformation in the unnotched bar. A possible geometry for a specimen is given in Fig. 2. The notch radius is variable and allows the selection of different degrees of multiaxial loading. The notch radius should be large enough to allow a correct measure of the lateral contraction at the notch tip. However, it should not be too large to avoid excessively shallow notches.

For specimens with a minimum diameter of 10 mm, notch roots of 2, 4, and 10mm, respectively are proposed for ferritic steels according to [12], while scaling to smaller sizes (down to 50%) is explicitely permitted.

For F82Hmod and EUROFER97 characterization, a minimum diameter of 5 mm, and notch roots of 1, 2, and 5mm, respectively are used [29]. For geometries other than those recommended in [12], selection of suitable notch geometries has to be done according to elastic-plastic analysis of stress fields and plastic zone evalution until fracture. In order to avoid effects from notch root finishing and to ensure that fracture is initiating from locations well inside the material, the final geometries should be selected in a way that, for stresses near to fracture, the axial stress in the plane perpendicular to the specimen axis at the notch root attains its maximum at the specimen interior. Also the course of the axial and circumferential stresses as well as the degree of multiaxiality in that plane should vary significantly for the various geometries.

2.1.2 Specimen preparation

All dimensions should be machined with sufficient accuracy. Ref. [12] states an accuracy of +0, -0.05mm for the minimum diameter and an accuracy of +/-0.02mm for the diameter. Finishing of the notch root has to be performed in axial direction to avoid surface defects that may trigger premature failures. At least 10 specimens should be tested per specimen geometry. To reduce statistical scatter of the results, however, a sample size of 20 specimens is more appropriate. All specimens have to be measured in order to ensure identical specimen dimensions and meeting of tolerance requirements.

2.1.3 Experimental procedure

Two parameters shall be continuously recorded during the test: load and diametral contraction across the minimum section. This can be achieved using extensometer or optical equipment. The test is performed under displacement control at 0.5 mm/min or under diametral strain control.

The final diameter of the broken specimen must be given. This can be measured after fracture. If the values obtained from the broken specimens for two perpendicular directions according to the main fabrication directions disagree, the presence of anisotropy must be mentioned in the report. Otherwise, the extensometer/optical recordings are assumed to be correct.

The temperature must be controlled to be within +/- 2° C for the notch.

The fractured surfaces should be photographed and kept for further inspection. A fractographic inspection of the fracture surfaces should be performed.

2.1.4 Reporting of the results

The precise initial dimensions must be stated. (Specimen ID, nominal notch radius, specimen diameter, diameter of the minimum section, actual notch radius)

The following results have to be reported for each specimen: Specimen ID, nominal notch radius, specimen diameter at fracture, load at fracture initiation, average fracture strain, average fracture stress, Weibull stress at fracture. Additionally, the Weibull modulus, the characteristic Weibull stress, and the selected unit volume have to be reported for the complete sample. These quantities are obtained from the numerical analysis of the test results (see 2.2).

As a result of the fractographic inspection, fracture origin locations and fracture appearance should be reported for each specimen. If this is not feasible, all specimens with average fracture strain levels below 3% and above 30% should be rejected [12].

2.2 Finite Element Analysis

Any standard finite element code capable of nonlinear structural analysis for elastic-plastic material behaviour may be used for the analysis. For the Finite Element Analysis of the stress field at fracture, the diameter reduction Δd between initial and final diameter measured at the notch root is used as loading variable. Each sample of specimens thus corresponds to a sample of Δd-values. For each of the Δd-values, a complete FE stress analysis is obtained.

2.2.1 Meshing and boundary conditions

An axisymmetrical 2-D model of the notched round bar geometry is appropriate. Due to symmetry reasons only half of the specimen has to be modelled. Axisymmetric isoparametric quadratic elements with 8 nodes and reduced integration are recommended for the analysis. Details of the finite element meshing are up to the user. As a rule of thumb, a minimum number of 8-10 elements at the notch section ($z = 0$) is required and the size of the element at the notch root should be sufficiently small to catch the notch stress distribution with reasonable accuracy.

Boundary conditions due to symmetry are:

$$u_z = 0 \text{ at } z = 0 \text{ and } u_r = 0 \text{ at } r = 0 \tag{23}$$

Loading can be applied by prescribed z-displacement boundary conditions for the nodes at $u_z = xx$, where xx denotes the displacement pickup location in the experiments (this needs not necessarily be so but facilitates comparison to experimental results!!!). The distance xx has to be sufficiently large to prevent inhomogeneous axial stresses due to the notch influence.

The applied force, F_f, at fracture is calculated from the axial stresses at $u_z = xx$. The diameter reduction Δd at fracture corresponds to 2 times the radial displacement of the node located at the notch root. The factor of 2 has to be applied for symmetry reasons (only the half section of the specimen is modelled in the FE axisymmetrical analysis).

The calculated $F - \Delta d$ curve has to meet the experimentally observed load-displacement curve (see for example Figures 3, 4). If this is not the case, a check of the material parameters and/or the meshing is necessary.

It has to be ensured that the calculated Δd-values coincide with the experimentally obtained diametral contractions at fracture which have been obtained by suitable measurements (e.g. optical or extensometer-based). In a first step, this can be obtained by choosing sufficiently small load increments in the FE analysis. Additional steps may be necessary with suitably adjusted z-displacement boundary conditions in order to achieve sufficiently accurate Δd-values.

2.2.2 Output requests

Mesh geometry and nodal displacements are required for the subsequent analysis. For the calculation of the cleavage fracture parameters, output of the principal stresses is required at the integration points of each element for each sample value of Δd at fracture.

Note: Within the ABAQUS FE code [1], this is achieved by

```
*EL FILE, POS=INTEGRATION POINTS
PS
```

2.2.3 Postprocessing

For the Weibull stress calculation, postprocessing of the Finite Element stress output is necessary. At each of the increasing fracture load levels characterized by increasing absolute values of Δd, the maximum value of the first principal stress at each integration point is identified and retained for subsequent use in Weibull stress calculation. A postprocessing routine `WEISTRABA` [27] is available for this purpose if the FE code ABAQUS [1] is used. It is useful to generate a result file containing only the necessary quantities (i.e. meshing information and principal stress envelopes at fracture) for the subsequent Weibull stress calculation. In the routine `WEISTRABA`, this file is called the `*.wst`-file.

2.3 Weibull stress calculation

The Weibull stress σ_W is obtained from the `*.wst`-file by numerical integration. For numerical reasons, the integration of the Weibull stress according to eq. (12) is performed after normalizing σ_1 by a suitably chosen reference stress, e.g. the flow stress. This is done to avoid numerical difficulties resulting from large values of the Weibull exponent m which is typically in the range of 10-30. The correction is removed after the numerical integration is complete. Eq. (12) then reads:

$$\left(\frac{\sigma_W}{\sigma_{\text{ref}}}\right)^m = \frac{1}{V_0}\int_{V_{pl}} \left(\frac{\sigma_1}{\sigma_{\text{ref}}}\right)^m \mathrm{d}V \tag{24}$$

and final correction is simply made by multiplying the resulting integral value by the value of the reference stress σ_{ref}^m.

Stresses are given at the integration points of the ABAQUS elements. Reduced integration is used, which means that we have 2x2=4 integration points per element in the 2D

case and 2x2x2=8 integration points in 3D problems. The Weibull stress is integrated element-by-element. In the general case of a 3D model, we have

$$\sigma_W = \sigma_{\text{ref}} \left[\frac{1}{V_0} \sum_{\text{el}} \sigma_{W_{\text{el}}} \right]^{\frac{1}{m}} \quad \text{with the auxiliary quantity of}$$

$$\sigma_{W_{\text{el}}} = \sum_{i=1}^{k_i} w_i \sum_{j=1}^{k_j} w_j \sum_{k=1}^{k_k} w_k \left(\frac{\sigma_1(r_i, s_j, t_k)}{\sigma_{\text{ref}}} \right)^m (\det J(r_i, s_j, t_k)) \qquad (25)$$

where k_i, k_j, k_k the number of integration points in each dimension and w_i, w_j, w_k the respective weights for the Gaussian integration. r_i, s_j, t_k are the coordinates in the FE natural element and $\det J(.)$ is the determinant of the Jacobi matrix for the transformation from the global to the natural element at the natural coordinates r_i, s_j, t_k.

The contributions from each element are summed up to give the final result. For $k_i = k_j = k_k = 2$, we have $w_i = w_j = w_k = 1$ and r_i, r_j, $r_k = 1/\sqrt{3}$.

2.3.1 Plastic zone size

A plastic zone indicator flag is used to extend numerical integration only over the plastic zone and not over the entire volume of the specimen. This plasticity flag is set to 1 for each integration point where plasticity occurs (in terms of a von Mises yield criterion or by checking the plastic strains of the FE output) and 0 otherwise. Any averaging procedures are avoided. Only the stress values at the integration points, which are known to be the most exact values within an element [3], are used.

For each FE load step, corresponding to a specimen fracture event, the first principal stress values are checked against the values of the previous step and a stress envelope is constructed to take into account locally decreasing stresses due to stress redistribution which may lead to decreasing values of the local risk of rupture.

2.3.2 Symmetry factor

If only part of the specimen is analysed for symmetry reasons, the calculated value of the Weibull stress has to be adjusted according to

$$\sigma_W \rightarrow \sigma_W * sym^{(\frac{1}{m})} \qquad (26)$$

where *sym* is the symmetry factor reflecting applied symmetry conditions. If e.g. only half of the geometry is modelled, $sym = 2$. For axisymmetric configurations, the symmetry factor may depend on the Finite Element code, i.e. whether a full 2π thickness or just a "unit thickness" of 1 rad is used. (For a "unit thickness" of 1 rad, $sym = 2 * 2\pi$ rad for the axisymmetric half-geometry configuration considered).

2.3.3 Unit volume

Weibull stress values and the parameter σ_u of the Weibull stress distribution are affected by different choices of the numerical value for the unit volume V_0. Some authors use V_0-values that are linked to microstructural length scales. A scaling procedure allows conversion, if V_0, as in the present context, is taken as arbitrary reference volume for the statistical model: $V_0 = 1\text{mm}^3$. Let V_0 and $\widetilde{V_0}$ be two differently taken reference volume values. Then, the respective values of σ_W and $\widetilde{\sigma_W}$ are given by

$$\widetilde{\sigma_W} = \left(\frac{V_0}{\widetilde{V_0}}\right)^{\frac{1}{m}} \sigma_W \tag{27}$$

with the Weibull modulus m as obtained by the maximum likelihood estimation procedure.

2.3.4 Local risk of rupture

The local risk of rupture [28] is defined as the probability of fracture starting from some sub-volume, V_s of the specimen, i.e. as the conditional probability of having a micro-crack in the sub-volume, V_s under the condition that this micro-crack causes unstable fracture. At a given load level i characterized by a Weibull stress value of $\sigma_W(i)$ the local risk of rupture at $\vec{x}$ is given by

$$\pi_i(\vec{x}|\sigma_W) = \frac{\sigma_1^m(\vec{x},\ i)}{V_0 \sigma_W^m(i)} \tag{28}$$

which can be integrated over the whole Weibull stress range to give the integrated local risk of rupture:

$$\pi(\vec{x}) = \int_0^\infty \pi_i(\vec{x}|\sigma_W)\, f_{\sigma_W}(\sigma_W) \mathrm{d}\sigma_W \tag{29}$$

with $\pi_i(.)$ as given in Eqn. 28 and the probability density $f_{\sigma_W}(.)$ of the Weibull stress at fracture. Eqn. 29 can be solved by numerical integration. An appropriate upper limit

of the integration domain can be selected by checking if the normalization condition $\int_V \pi(\vec{x})\mathrm{d}V = 1$ is satisfied.

The quantity $\pi(.)$ predicts the fracture initiation location distribution that is accessible via fractographic identification of fracture origin locations. Within the postprocessor `WEISTRABA`, values of $\pi(.)$ are available at each integration point of the finite element model and graphical visualization is obtained by the graphical visualization package FEMVIEW.

A comparison of $\pi(.)$ with experimental values for the fracture origin distribution can be used to verify if the numerical approach to fracture description is appropriate. This is especially useful for transferability predictions to different geometries.

2.4 Fractography

Fractography is an essential part of the procedure. All of the fractured specimens should be qualitatively (fracture appearance) and quantitatively (fracture origin location) investigated. A first assessment of the fracture appearance can be performed using a light microscope. For a thorough analysis, use of SEM is recommended. Fractographic analysis gives a justification of the appropriateness of analysis in that it is able to identify the relevant micromechanisms that are responsible for the fracture process.

2.4.1 Fracture appearance

Fracture appearance should be classified as trans- or intercrystalline cleavage with or without ductile parts. Fracture origins, if detectable, should be identified as visible. The presence of particles at the fracture initiation sites should be mentioned and the nature of the particles should be identified.

2.4.2 Fracture origin distribution

For each of the specimens, the location of the fracture initiation sites that are detected should be given. It is preferable to give the location with respect to the specimen centre that has to be identified. A table of the fractographic results should contain the following entries: specimen No., fracture appearance characterization, cleavage initiation inclusion classification (size and kind), presence and size of ductile islands, distance of fracture initiation site to specimen axis.

Availability of fracture origin distribution data is the key issue for comparison between experimental results and numerical analysis and justification of numerical approach via local risk of fracture assessment.

3 Evaluation rules; Statistical inference

As indicated in the previous paragraphs, the Weibull stress depends on the Weibull modulus m which in turn is a result of the statistical analysis of the Weibull stress values of the fractured specimens. As shown in Ref. [21], an iterative procedure is required for the determination of the distribution parameters of the Weibull stress, namely m and σ_u. In a first step, starting from a suitable value of the Weibull modulus, e.g. $m = 20$, a preliminary sample of Weibull stress values is calculated. From this sample, the distribution parameters m and σ_u are determined using Maximum Likelihood procedure. If m differs not too much from the previous value, the procedure is terminated, otherwise it is repeated with the new value of m until convergence is attained which is usually the case after few (2-5) iterations.

After convergence is attained, the maximum likelihood estimates are used to calculate 90%-confidence intervals. Two alternative methods are possible: Maximum likelihood based confidence intervals according to the procedure in [8] and confidence intervals based on resampling or bootstrap methods [30].

3.1 Determination of the Weibull parameters

The determination of the two parameters m and σ_u has to be performed iteratively as σ_W depends on the (unknown) parameter m.

Step 1: Use a starting value of $m = 20$ and calculate the Weibull stress σ_W at fracture for each fractured specimen as described in Section 2.3.

Step 2: Rank the results in increasing order of Weibull stress σ_W. Plot $\ln\ln[\frac{1}{1-\overline{F(x_n)}}]$ as a function of $\ln x_{(n)}$, where $x_{(n)}$ is the Weibull stress of the specimen with rank n and $\overline{F(x_n)} = \frac{n}{N+1}$ is the mean (cumulative) frequency of the n-th observation (using $\frac{n}{N+1}$ as plotting position is generally recommended for statistical reasons – e.g. [13] –, although it plays no role if the maximum likelihood method is used for parameter estimation). As the theoretical relation between failure probability and σ_W is given by

$$P_f = 1 - \exp\left[-\left(\frac{\sigma_W}{\sigma_u}\right)^m\right] \quad , \tag{30}$$

a plot of $\ln\ln[\frac{1}{1-\overline{F(x_n)}}]$ versus $\ln\sigma_{W(n)}$, where $\sigma_{W(n)}$ is the "experimental" Weibull stress for the specimen with rank n, should give an approximately linear relation. (Step 2 is only recomended for visualization purposes and is not necessary for Step 3)

Step 3: Use the maximum likelihood method to determine the parameters m and σ_u of the Weibull distribution of the Weibull stress. The maximum likelihood estimators of m and σ_u are denoted by $\hat{m}$ and $\widehat{\sigma_u}$, respectively. $\hat{m}$ is the solution of the nonlinear equation

$$\frac{N}{\hat{m}} + \sum_{i=1}^{N} \ln \sigma_{W_{(i)}} - N \frac{\sum_{i=1}^{N} \sigma_{W_{(i)}}^{\hat{m}} \ln \sigma_{W_{(i)}}}{\sum_{i=1}^{N} \sigma_{W_{(i)}}^{\hat{m}}} = 0 \tag{31}$$

which can be obtained by any suitable numerical procedure. Using $\hat{m}$, the maximum likelihood estimator $\widehat{\sigma_u}$ is obtained from the equation

$$\widehat{\sigma_u} = \left(\frac{1}{N} \sum_{i=1}^{N} \sigma_{W_{(i)}}^{\hat{m}} \right)^{\frac{1}{\hat{m}}} \tag{32}$$

Correct $\hat{m}$ with the unbiasing factor $b(N)$ given in Table 1: $\hat{m}_{unb} = \hat{m} * b(N)$.

Step 4: If the maximum likelihood estimators $\widehat{\sigma_u}$ and $\hat{m}_{unb}$ agree within a fixed tolerance with those of the previous iteration, their values are considered acceptable. Otherwise, repeat steps 2-4. A flow diagram is given in Figure 5 to illustrate the iterative procedure.

3.2 Confidence intervals for m and σ_u based on maximum likelihood estimators

Confidence intervals for the Weibull parameters m and σ_u determined by the maximum likelihood method are obtained with the following procedure:

1. Select a confidence level $1-2\alpha$ (usually 90% or 95%, i.e. $\alpha = 0.05$ or $\alpha = 0.025$).
   Set $\alpha_1 = \alpha$ and $\alpha_2 = 1-\alpha$.

2. Take $t_1(N, \alpha_1)$ and $t_2(N, \alpha_2)$ from Table 2.
   Calculate $A = \widehat{\sigma_u} * \exp(-t_2/\hat{m})$ and $B = \widehat{\sigma_u} * \exp(-t_1/\hat{m})$.
   Report $[A, B]$ as the confidence interval for σ_u for a confidence level of $1-2\alpha$.

3. Take $l_1(N, \alpha_1)$ and $l_2(N, \alpha_2)$ from Table 3.
   Calculate $C = \hat{m}/l_2$ and $D = \hat{m}/l_1$.
   Report $[C, D]$ as the confidence interval for m for a confidence level of $1-2\alpha$.

These quantities have to be calculated with the maximum likelihood estimate of m without the unbiasing factors.

The Maximum Likelihood confidence intervals of the Weibull parameters shall be reported as shown in Table 4:

Note: The confidence intervals for m and σ_u are valid only if $\hat{m}$ and $\widehat{\sigma_u}$ were obtained by the maximum likelihood method. Any other estimation procedure for the Weibull parameters yields different confidence intervals. [2]

The Tables 1, 2 and 3 were taken from Ref. [36] and are also contained in [8]. It should be noted, that the confidence intervals obtained in this way are not strictly valid for the iterative Weibull parameter estimation procedure.

Presentation of the results shall be made in a graph according to Figure 6 with suitably adjusted range of horizontal axes. The calculated values for $\ln\sigma_W$ are plotted together with the Weibull distribution, which is a line with the slope $\hat{m}$ and containing the point $(\widehat{\sigma_u}, 0)$.

3.3 Bootstrap confidence intervals

It should be emphasized that the evaluation of the distribution parameters of σ_W, namely m and σ_u, is based on statistical inference methods that are applied without fully meeting the conditions of their applicability. It is not clear beforehand whether the maximum likelihood parameter estimation gives valid results for the present case, where the random variate depends on the distribution parameter itself and an iterative procedure is used to obtain consistent results. There are no methods available to quantify the statistical properties of the estimators of the Weibull parameters.

For these reasons, the confidence intervals based on the results found by Thoman et al. [36] and used in the ESIS P6 procedure [12] may only approximately reflect the statistical uncertainty of the parameter estimates. This situation is completetly different from the Weibull parameter estimation in the strength measurement for ceramics (see [8]), where no iterative procedure is required.

Alternative ways for confidence intervals which do not suffer from these restrictions are given by so-called bootstrap methods.

3.3.1 Bootstrap simulation procedure

In the following, a *very* concise description of the bootstrap method mainly based on [11] is given. (We use the common statistical nomenclature, hats ($\hat{\cdot}$) denote estimates,

[2] An EXCEL template for the purpose of (non-iterative) Weibull parameter evaluation is available upon e-mail request to: riesch-oppermann@imf.fzk.de. Iterative Weibull parameter evaluation is contained in the `WEISTRABA` code available at the same address.

asterisks ($.^*$) denote quantities related to bootstrap samples; n is the sample size, B is the number of bootstrap simulations.)

Suppose we observe $x_1, \ldots, x_n$ independent data points, from which we compute a statistic of interest $s(x_1, \ldots, x_n)$.

A *bootstrap sample* $x^* = (x_1^*, \ldots, x_n^*)$ is obtained by randomly sampling, n times, with replacement, from the original data points $x_1, \ldots, x_n$. If this is repeated B times, we can generate a large number of independent bootstrap samples $x^{*1}, \ldots, x^{*B}$, each of size n.

Corresponding to each bootstrap sample x^{*b} there is a bootstrap replication of s, namely $s(x^{*b})$, the value of the statistic of interest computed for sample x^{*b}.

As a result, we obtain a bootstrap estimate for the statistic of interest:

$$s(.) = \sum_{b=1}^{B} s(x^{*b})/B \tag{33}$$

together with a bootstrap estimate for its standard deviation, namely

$$\widehat{\text{se}}_{\text{boot}} = \left\{ \frac{1}{B-1} \sum_{b=1}^{B} \left[s(x^{*b}) - s(.) \right]^2 \right\}^{\frac{1}{2}} \tag{34}$$

where $s(.) = \sum_{b=1}^{B} s(x^{*b})/B$ is the mean value of the statistic s after B bootstrap simulations defined in Eq. (33).

Note: In the present case, the statistic of interest consists of the pair $(m,\ \sigma_u)$ given in Eqs. (31) and (32), respectively.

3.3.2 Bootstrap confidence interval calculation

Using $\widehat{\text{se}}_{\text{boot}}$ and $s(.)$, it is possible to attribute confidence intervals to bootstrap estimates $\hat{\theta}^*(.) = \sum_{b=1}^{B} \hat{\theta}^*(b)/B$, where $\hat{\theta}^*(b) = s(x^{*b})$ is the bootstrap replication of $\hat{\theta} = s(x_1, \ldots, x_n)$ as defined above. For example, we obtain the usual standard normal $(1-2\alpha)$-confidence interval for θ, which is

$$\hat{\theta} \pm z^{(\alpha)} \times \widehat{\text{se}} \tag{35}$$

where $z^{(\alpha)}$ is the α-quantile of a standard normal distribution, e.g. $z^{(0.95)} = 1.645$ for the 90% confidence intervals. This leads to the so-called *standard bootstrap confidence intervals* which still rely on normal theory assumptions as can be seen from Eq. (35), which only holds exactly if $\hat{\theta}$ follows a normal distribution.

But it is also possible to obtain accurate confidence intervals for non-normally distributed statistics, i.e. without relying on normal theory assumptions. This is done by using $\hat{G}$, the cumulative distribution of the bootstrap replications $\hat{\theta}^*$. The $1-2\alpha$ *percentile interval* for θ is defined by the α- and $(1-\alpha)$-quantiles of $\hat{G}$. From B independent bootstrap samples, we obtain the percentile confidence intervals by taking the $B\times\alpha$th value in the ordered list of the B bootstrap replications of $\hat{\theta}^*$ as the lower limit and the $B\times(1-\alpha)$th value of the list as the upper limit of the confidence interval. These empirical percentiles are denoted $\hat{\theta}_B^{*(\alpha)}$ and $\hat{\theta}_B^{*(1-\alpha)}$ respectively and the percentile confidence interval reads

$$[\hat{\theta}_B^{*(\alpha)},\ \hat{\theta}_B^{*(1-\alpha)}] \tag{36}$$

for a confidence level of $1-2\alpha$.

Some drawbacks of the percentile intervals with respect to coverage probabilities are handled by an improved version of the percentile method including bias correction in the bootstrap replications. Bias correction z_0 is obtained from the cumulative distribution function $\hat{G}$ of the bootstrap replication and the original estimate $\hat{\theta}$ of the original sample via

$$z_0 = \Phi^{-1}(\hat{G}(\hat{\theta})) \tag{37}$$

where $\Phi^{-1}(.)$ is the inverse standard normal cumulative distribution function (CDF). We obtain the bias-corrected bootstrap confidence intervals as

$$\left[\hat{G}^{-1}\left(\Phi(2z_0+\Phi^{-1}(\alpha))\right),\ \hat{G}^{-1}\left(\Phi(2z_0+\Phi^{-1}(1-\alpha))\right)\right] \tag{38}$$

with z_0 from Eq. (37). Figure 7 contains the necessary auxiliary quantities and indicates how the bias-corrected bootstrap confidence intervals are obtained.

3.3.3 Reporting of bootstrap confidence intervals

Confidence intervals for the Weibull parameters m and σ_u determined by the bootstrap method are obtained with the following procedure:

1. Select a confidence level $1-2\alpha$ (usually 90% or 95%, i.e. $\alpha=0.05$ or $\alpha=0.025$).
   Set $\alpha_1=\alpha$ and $\alpha_2=1-\alpha$.

2. Perform B bootstrap simulations and obtain the empirical CDF $\hat{G}(.)$ of $\hat{m}^*$ and $\widehat{\sigma_u}^*$, respectively.
   Obtain the empirical percentiles $\hat{m}_B^{*(\alpha_1)}$ and $\hat{m}_B^{*(\alpha_2)}$ and $\hat{\sigma}_{uB}^{*(\alpha_1)}$ and $\hat{\sigma}_{uB}^{*(\alpha_2)}$.

3. Calculate the bias correction z_0 for σ_u(see Eq. 37): $z_0 = \Phi^{-1}(\hat{G}(\hat{\sigma_u}))$.
   Calculate $A = \hat{G}^{-1}\left(\Phi(2z_0 + \Phi^{-1}(\alpha_1))\right)$ and $B = \hat{G}^{-1}\left(\Phi(2z_0 + \Phi^{-1}(\alpha_2))\right)$.
   Report $[A, B]$ as the confidence interval for σ_u for a confidence level of $1 - 2\alpha$.

4. Calculate the bias correction z_0^m for m (see Eq. 37): $z_0^m = \Phi^{-1}(\hat{G}(\hat{m}))$.
   Calculate $C = \hat{G}^{-1}\left(\Phi(2z_0^m + \Phi^{-1}(\alpha_1))\right)$ and $D = \hat{G}^{-1}\left(\Phi(2z_0^m + \Phi^{-1}(\alpha_2))\right)$.
   Report $[C, D]$ as the confidence interval for m for a confidence level of $1 - 2\alpha$.

The bootstrap confidence intervals of the Weibull parameters shall be reported as shown in Table 5.

4 Validation/limits

The procedure was tested and verified within an ESIS Round Robin on Numerical Modelling [26]. Correct implementation of the cleavage fracture model was confirmed. It turned out, however, that modelling of the stress analysis and the subsequent statistical analysis of the results requires some skill in the choice of appropriate boundary conditions which may be source of large deviations in the resulting cleavage fracture parameters.

Validation using F82Hmod data was done using circumferentially notched tensile specimens. A limited number of results was obtained from pre-cracked axisymmetric tensile specimens. Validation using EUROFER data was done using circumferentially notched specimens. For both materials, fractography revealed a limited domain of applicability of the pure cleavage fracture model.

A detailed summary of the verification results is contained in a companion report [29].

Limits for cleavage fracture modelling are related to presence of different fracture mechanisms and violation of the basic assumptions described in Section 1.2. Presence of different fracture mechanisms may be related to different temperature regimes and/or irradiation effects. Violation of basic assumptions may be due to steep stress gradients as e.g. related to thermal shock loading or in pre-cracked specimens, where the fracture mechanics failure model according to Eq. 1 is inappropriate and has to be extended [30].

5 Status notes

This document contains the basic analysis procedure for a fracture mechanics assessment of failure of RAFM in the lower shelf regime based on the Local Approach to cleavage fracture.

Application of Local Approach methods requires a combination of different methods: experimental, numerical, statistical, and fractographic analysis steps are necessary.

Local Approach methods and their application are a subject of ongoing research. The methods described in this document are well established and applied to a number of large-scale test evaluation programmes for reactor pressure vessel steels.

Open questions remain with respect to their unmodified applicability to RAFM steels. Here, issues of strain-induced anisotropy seem to play an important role as crack initiation mechanism.

Acknowledgement

This report covers work performed within the framework of the Nuclear Fusion Programme of the Forschungszentrum Karlsruhe.

Support of the European Community via the 5th framework Fusion Technology Programme under task ID TTMS-005 is gratefully acknowledged.

Part of the numerical methods have been developed within the context of a center of collaborative research at Karlsruhe University (SFB483) for which financial support of the Deutsche Forschungsgemeinschaft is appreciated.

References

[1] ABAQUS/Standard User's Manual (Version 5.8), Hibbit, Karlsson & Sorensen, Inc. 1998.

[2] E. Amar, A. Pineau, Application of a Local Approach to Ductil-Brittle Transition in a Low-Alloyed Steel, Nuclear Engineering and Design **105** (1987), 89-96.

[3] K.-J. Bathe, Finite Element Procedures in Engineering Analysis, Prentice-Hall, Englewood Cliffs, NJ 1982.

[4] F.M. Beremin, A local criterion for cleavage fracture of a nuclear pressure vessel steel, Met. Trans. **14A** (1983), 2277-2287.

[5] F.M. Beremin, Cavity formation from inclusions in ductile fracture of A508 steel, Met. Trans. **12A** (1981), 723-732.

[6] British Energy Generation Ltd., Assessment of the integrity of structures containing defects - Revision 4, 2001.

[7] A. Brückner-Foit, W. Ehl, D. Munz, B. Trolldenier, The size effect and microstructural implications of the weakest link model, Fatigue Fract. Engng Mater. Struct. **13** (1990), 185-200.

[8] European Standard ENV 843-5, Advanced monolithic ceramics - mechanical tests at room temperature - statistical analysis.

[9] E 399 - 90 (1997), Standard Test Method for Plane Strain Fracture Toughness of Metallic Materials, ASTM, Annual Book of ASTM Standards, Vol. 03.01., 2001, 1119-1135.

[10] E 1921 - 97, Standard Test Method for Determination of Reference Temperature, T_0, for Ferritic Steels in the Transition Range, ASTM, Annual Book of ASTM Standards, Vol 03.01., 2001, 1119-1135.

[11] B. Efron, R.J. Tibshirani, An introduction to the bootstrap, Chapman & Hall, Boca Raton, 1993.

[12] ESIS P6 - 98, Procedure to Measure and Calculate Local Approach Criteria Using Notched Tensile Specimens, ESIS Document, European Structural Integrity Society, March 1998.

[13] E.J. Gumbel, Statistics of Extremes, Columbia University Press, 1958.

[14] G.T. Hahn, The Influence of Microstructure on Brittle Fracture Toughness, Met. Trans **15A** (1984), 947-959.

[15] K. Hojo, I. Muroya, A. Brückner-Foit, Fracture toughness transition curve estimation from a notched round bar specimen using the local approach method, Nuclear Engineering and Design **174** (1997), 247-258.

[16] Y. Huang, Accurate Dilatation Rates for Spherical Voids in Triaxial Stress Fields, J. Appl. Mech. **58** (1991), 1084-1086.

[17] A.L. Gurson, Continuum Theory of Ductile Rupture by Void Nucleation and Growth: Part I - Yield Criteria and Flow Rules for Porous Ductile Media, J. Engng Mat. Tech. **99** (1977), 2ff.

[18] G.T. Hahn, R.G. Hoagland, A.R. Rosenfield, The Variation of K_{Ic} with Temperature and Loading Rate, Met. Trans. **2** (1971), 537-541.

[19] E. Kantidis, B. Marini, L. Allais, A. Pineau, Validation of a statistical criterion for intergranular brittle fracture of a low alloy steel through uniaxial and biaxial (tension-torsion) tests, Int. J. Fracture **66** (1994), 273-294.

[20] J.D. Landes, D.H. Shaffer, Statistical Characterization of Fracture in the Transition Region, in: Fracture Mechanics: Twelfth Conference, ASTM STP 700, American Society for Testing and Materials (1980), 368-382.

[21] F. Minami, A. Brückner-Foit, D. Munz, B. Trolldenier, Estimation procedure for the Weibull parameters used in the local approach, Int. J. Fract. **54** (1992), 197-210.

[22] F. Mudry, A local approach to cleavage fracture, Nucl. Engng. and Des. **105** (1987), 65-76.

[23] F. Mudry, F. di Rienzo, A. Pineau, Numerical Comparison of Global and Local Fracture Criteria in Compact Tension and Center-Crack Panel Specimens, in: J.D. Landes, A. Saxena, J.G. Merkle (eds.), Nonlinear Fracture Mechanics: Vol. II - Elastic-Plastic Fracture, ASTM STP 995 (1989), 24-39.

[24] H.G. Pisarski, K. Wallin, The SINTAP fracture toughness estimation procedure, Engineering Fracture Mechanics **67** (2000), 613-624.

[25] J.R. Rice, D.M. Tracey, On the ductile enlargement of voids in triaxial stress fields, J. Mech. Phys. Solids **17** (1969), 201-217.

[26] H. Riesch-Oppermann, FZK Contribution to the ESIS TC 8 Numerical Round Robin on Micromechanical Models (Phase II, Task B1), FZKA Report 6338, Forschungszentrum Karlsruhe, 1999.

[27] H. Riesch-Oppermann, A. Brückner-Foit, WEISTRABA - A code for the numerical analysis of Weibull stress parameters from ABAQUS finite element stress analyses - Procedural background and code description -, FZKA Report 6155, Forschungszentrum Karlsruhe, August 1998.

[28] H. Riesch-Oppermann, E. Diegele, Towards a micro-mechanical description of the fracture behaviour for RAFM steels in the ductile-to-brittle transition regime, J. Nucl. Materials **307-311P2** (2003), 179-183.

[29] H. Riesch-Oppermann, E. Diegele, Verification of a fracture mechanics concept for the cleavage fracture behaviour of RAFM steels using local fracture criteria, FZKA Report 6794, Forschungszentrum Karlsruhe, (in preparation).

[30] H. Riesch-Oppermann, M. Walter, Status report on experiments and modelling of the cleavage fracture behaviour of F82Hmod using local fracture criteria: Task TTMS-005 , Report FZKA 6388, Forschungszentrum Karlsruhe, 2001.

[31] R.O. Ritchie, J.F. Knott, J.R Rice, On the relationship between critical tensile stress and fracture toughness in mild steels, J. Mech. Phys. Solids **21** (1973), 395-410.

[32] R.O. Ritchie, W.L. Server, R.A. Wullaert, Critical Fracture Stess and Fracture Strain Models for the Prediction of Lower and Upper Shelf Toughness in Nuclear Pressure Vessel Steels, Metall. Trans. **10A** (1979), 1557-1569.

[33] R.A. Rosenfield et al., What does the Charpy test really tell us? ASM, Metals Park, 1978.

[34] G. Rousselier, Ductile Fracture Models and their Potentials in Local Approach of Fracture, Nuclear Engineering and Design **105** (1987), 97-111.

[35] A.N. Stroh, The formation of cracks as a result of plastic flow, Proc. Roy. Soc. **212** (1954), 404-414.

[36] D.R. Thoman, L.J. Bain, C.E. Antle, Inferences on the Parameters of the Weibull Distribution, Technometrics, **11** (1969), 445-460.

A Figures

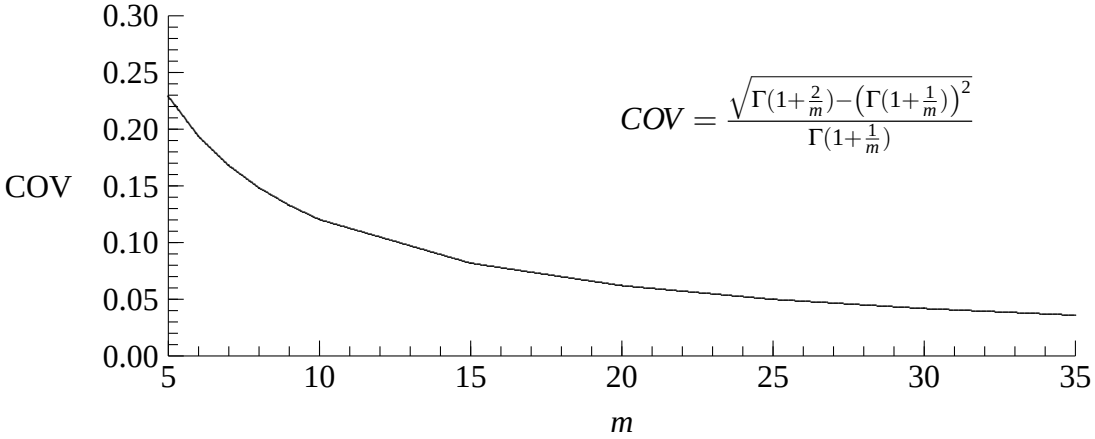

Figure 1: COV of Weibull distributed random variate for different moduli m.

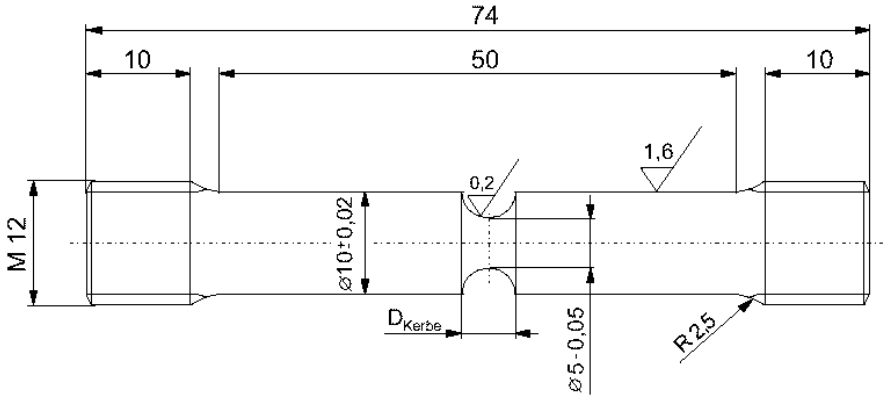

Figure 2: Geometry of axisymmetrically notched bar (RNB) specimens.

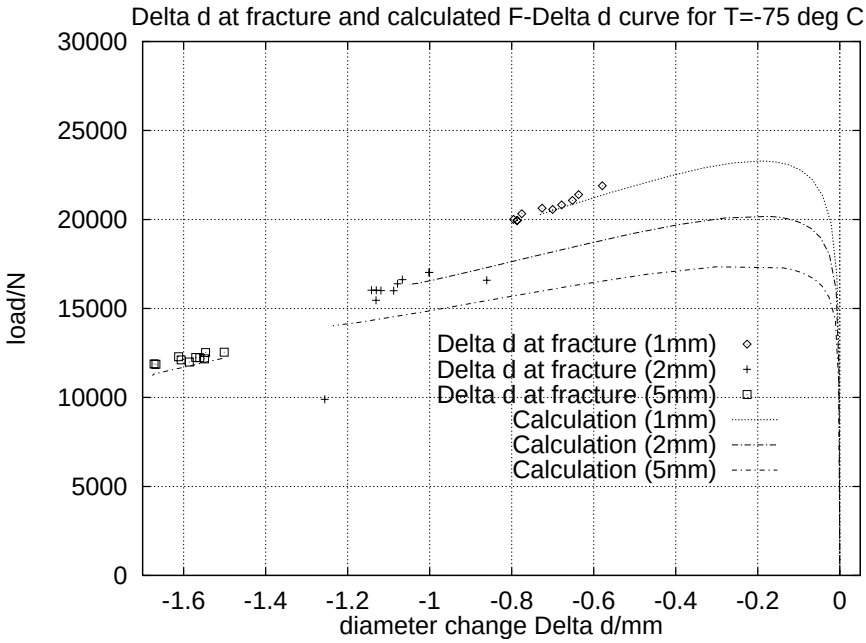

Figure 3: Calculated $F - \Delta d$-curves and experimental Δd at fracture (-75° C) for F82Hmod steel.

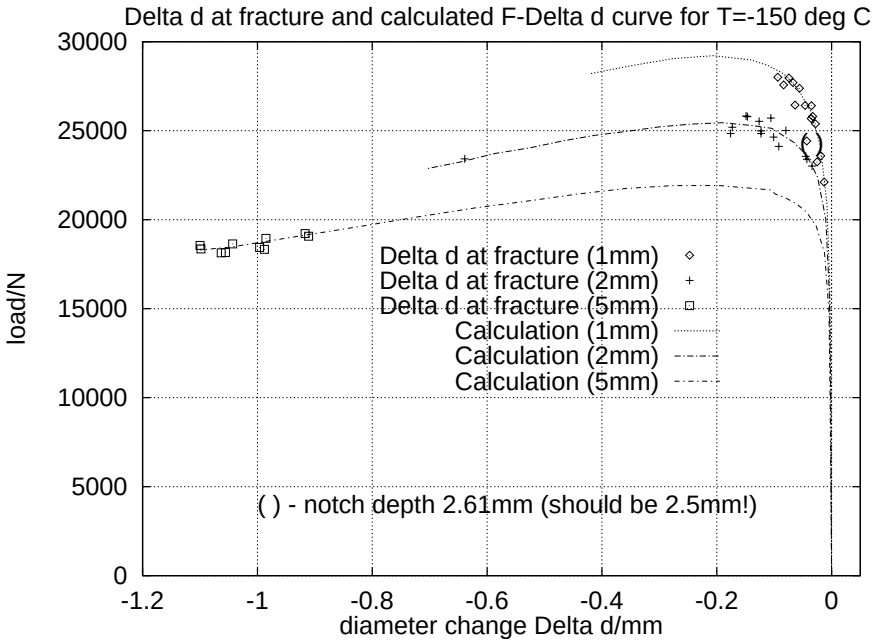

Figure 4: Calculated $F - \Delta d$-curves and experimental Δd at fracture (-150° C) for F82Hmod steel.

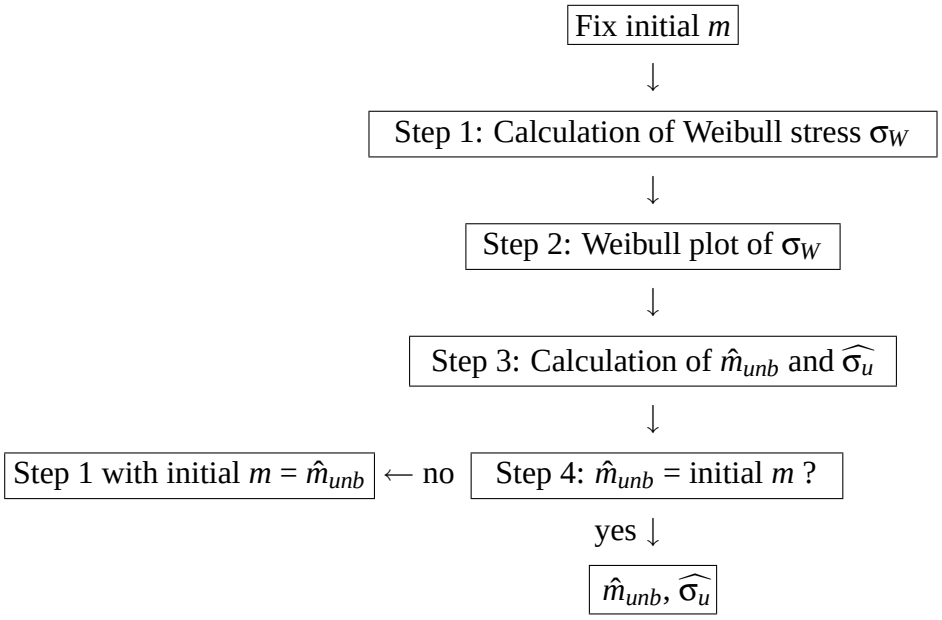

Figure 5: Flow diagram for iterative Weibull parameter estimation procedure.

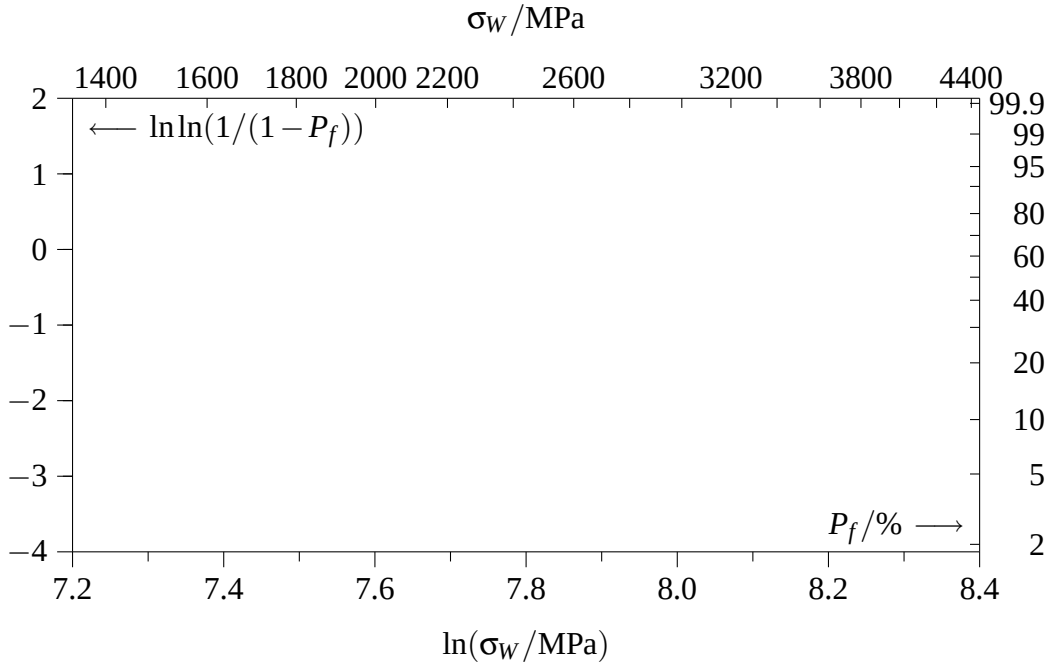

Figure 6: Template for Weibull plot of σ_W

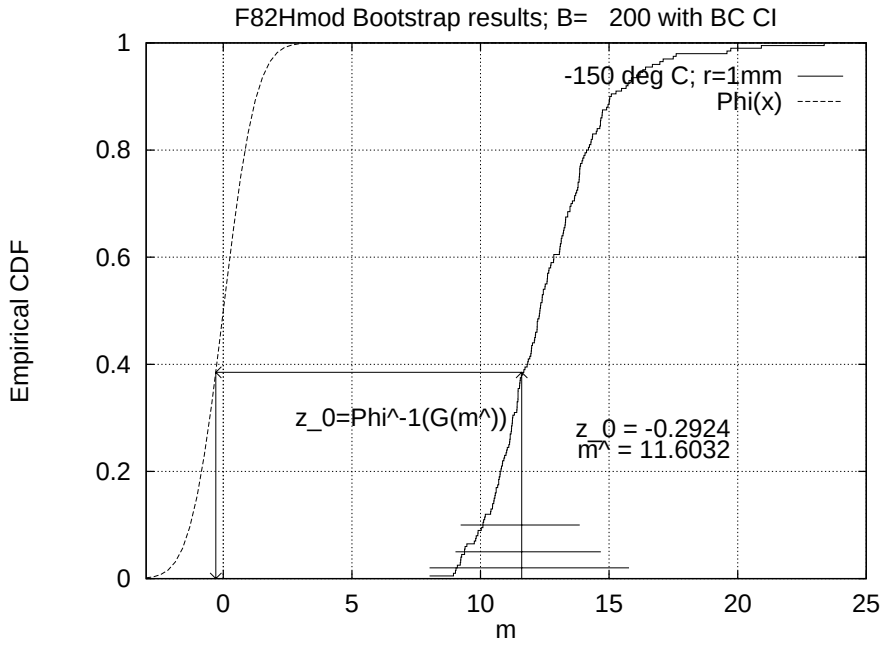

Figure 7: Bootstrap empirical CDF $\hat{G}(\hat{m}_B^*)$ for r=1mm notched specimens tested at -150° C. (Horizontal lines mark length of bias corrected bootstrap confidence intervals. Auxiliary arrows indicate how z_0^m is determined.)

B Tables

N	$b(N)$
5	0.669
6	0.752
7	0.792
8	0.820
9	0.842
10	0.859
11	0.872
12	0.883
13	0.893
14	0.901
15	0.908
16	0.914

N	$b(N)$
17	0.919
18	0.923
19	0.927
20	0.931
21	0.935
22	0.938
23	0.941
24	0.943
25	0.945
26	0.947
27	0.949
28	0.951

N	$b(N)$
29	0.953
30	0.955
31	0.957
32	0.958
33	0.959
34	0.960
35	0.961
36	0.962
37	0.963
38	0.964
39	0.965
40	0.966

Table 1: Unbiasing factors $b(N)$

N	$\alpha_1 = 0.02$	$\alpha_1 = 0.05$	$\alpha_1 = 0.10$	$\alpha_2 = 0.90$	$\alpha_2 = 0.95$	$\alpha_2 = 0.98$
5	-1.631	-1.247	-0.888	0.772	1.107	1.582
6	-1.396	-1.007	-0.74	0.666	0.939	1.291
7	-1.196	-0.874	-0.652	0.598	0.829	1.12
8	-1.056	-0.784	-0.591	0.547	0.751	1.003
9	-0.954	-0.717	-0.544	0.507	0.691	0.917
10	-0.876	-0.665	-0.507	0.475	0.644	0.851
11	-0.813	-0.622	-0.477	0.448	0.605	0.797
12	-0.762	-0.587	-0.451	0.425	0.572	0.752
13	-0.719	-0.557	-0.429	0.406	0.544	0.714
14	-0.683	-0.532	-0.41	0.389	0.52	0.681
15	-0.651	-0.509	-0.393	0.374	0.499	0.653
16	-0.624	-0.489	-0.379	0.36	0.48	0.627
17	-0.599	-0.471	-0.365	0.348	0.463	0.605
18	-0.578	-0.455	-0.353	0.338	0.447	0.584
19	-0.558	-0.441	-0.342	0.328	0.433	0.566
20	-0.54	-0.428	-0.332	0.318	0.421	0.549
22	-0.509	-0.404	-0.314	0.302	0.398	0.519
24	-0.483	-0.384	-0.299	0.288	0.379	0.494
26	-0.46	-0.367	-0.286	0.276	0.362	0.472
28	-0.441	-0.352	-0.274	0.265	0.347	0.453
30	-0.423	-0.338	-0.264	0.256	0.334	0.435
32	-0.408	-0.326	-0.254	0.247	0.323	0.42
34	-0.394	-0.315	-0.246	0.239	0.312	0.406
36	-0.382	-0.305	-0.238	0.232	0.302	0.393
38	-0.37	-0.296	-0.231	0.226	0.293	0.382
40	-0.36	-0.288	-0.224	0.22	0.285	0.371
42	-0.35	-0.28	-0.218	0.214	0.278	0.361
44	-0.341	-0.273	-0.213	0.209	0.271	0.352
46	-0.333	-0.266	-0.208	0.204	0.264	0.344
48	-0.325	-0.26	-0.203	0.199	0.258	0.336
50	-0.318	-0.254	-0.198	0.195	0.253	0.328
52	-0.312	-0.249	-0.194	0.191	0.247	0.321
54	-0.305	-0.244	-0.19	0.187	0.243	0.315
56	-0.299	-0.239	-0.186	0.184	0.238	0.309
58	-0.294	-0.234	-0.183	0.181	0.233	0.303
60	-0.289	-0.23	-0.179	0.177	0.229	0.297
62	-0.284	-0.226	-0.176	0.174	0.225	0.292
64	-0.279	-0.222	-0.173	0.171	0.221	0.287
66	-0.274	-0.218	-0.17	0.169	0.218	0.282
68	-0.27	-0.215	-0.167	0.166	0.214	0.278
70	-0.266	-0.211	-0.165	0.164	0.211	0.274

Table 2: Auxiliary variables for the confidence interval for σ_u

N	$\alpha_1 = 0.02$	$\alpha_1 = 0.05$	$\alpha_1 = 0.10$	$\alpha_2 = 0.90$	$\alpha_2 = 0.95$	$\alpha_2 = 0.98$
72	-0.262	-0.208	-0.162	0.161	0.208	0.269
74	-0.259	-0.205	-0.16	0.159	0.205	0.266
76	-0.255	-0.202	-0.158	0.157	0.202	0.262
78	-0.252	-0.199	-0.155	0.155	0.199	0.258
80	-0.248	-0.197	-0.153	0.153	0.197	0.255
85	-0.241	-0.19	-0.148	0.148	0.19	0.246
90	-0.234	-0.184	-0.144	0.143	0.185	0.239
95	-0.227	-0.179	-0.139	0.139	0.179	0.232
100	-0.221	-0.174	-0.136	0.136	0.175	0.226
110	-0.211	-0.165	-0.129	0.129	0.166	0.215
120	-0.202	-0.158	-0.123	0.123	0.159	0.205

Table 2: Auxiliary variables for the confidence interval for σ_u (cont'd.)

N	$\alpha_1 = 0.02$	$\alpha_1 = 0.05$	$\alpha_1 = 0.10$	$\alpha_2 = 0.90$	$\alpha_2 = 0.95$	$\alpha_2 = 0.98$
5	0.604	0.683	0.766	2.277	2.779	3.518
6	0.623	0.697	0.778	2.03	2.436	3.067
7	0.639	0.709	0.785	1.861	2.183	2.64
8	0.653	0.72	0.792	1.747	2.015	2.377
9	0.665	0.729	0.797	1.665	1.896	2.199
10	0.676	0.738	0.802	1.602	1.807	2.07
11	0.686	0.745	0.807	1.553	1.738	1.972
12	0.695	0.752	0.811	1.513	1.682	1.894
13	0.703	0.759	0.815	1.48	1.636	1.83
14	0.71	0.764	0.819	1.452	1.597	1.777
15	0.716	0.77	0.823	1.427	1.564	1.732
16	0.723	0.775	0.826	1.406	1.535	1.693
17	0.728	0.779	0.829	1.388	1.51	1.66
18	0.734	0.784	0.832	1.371	1.487	1.63
19	0.739	0.788	0.835	1.356	1.467	1.603
20	0.743	0.791	0.838	1.343	1.449	1.579
22	0.752	0.798	0.843	1.32	1.418	1.538
24	0.759	0.805	0.848	1.301	1.392	1.504
26	0.766	0.81	0.852	1.284	1.37	1.475
28	0.772	0.815	0.856	1.269	1.351	1.45
30	0.778	0.82	0.86	1.257	1.334	1.429
32	0.783	0.824	0.863	1.246	1.319	1.409
34	0.788	0.828	0.866	1.236	1.306	1.392
36	0.793	0.832	0.869	1.227	1.294	1.377
38	0.797	0.835	0.872	1.219	1.283	1.363
40	0.801	0.839	0.875	1.211	1.273	1.351

Table 3: Auxiliary variables for the confidence interval for *m*

N	$\alpha_1 = 0.02$	$\alpha_1 = 0.05$	$\alpha_1 = 0.10$	$\alpha_2 = 0.90$	$\alpha_2 = 0.95$	$\alpha_2 = 0.98$
42	0.804	0.842	0.877	1.204	1.265	1.339
44	0.808	0.845	0.88	1.198	1.256	1.329
46	0.811	0.847	0.882	1.192	1.249	1.319
48	0.814	0.85	0.884	1.187	1.242	1.31
50	0.817	0.852	0.886	1.182	1.235	1.301
52	0.82	0.854	0.888	1.177	1.229	1.294
54	0.822	0.857	0.89	1.173	1.224	1.286
56	0.825	0.859	0.891	1.169	1.218	1.28
58	0.827	0.861	0.893	1.165	1.213	1.273
60	0.83	0.863	0.894	1.162	1.208	1.267
62	0.832	0.864	0.896	1.158	1.204	1.262
64	0.834	0.866	0.897	1.155	1.2	1.256
66	0.836	0.868	0.899	1.152	1.196	1.251
68	0.838	0.869	0.9	1.149	1.192	1.246
70	0.84	0.871	0.901	1.146	1.188	1.242
72	0.841	0.872	0.903	1.144	1.185	1.237
74	0.843	0.874	0.904	1.141	1.182	1.233
76	0.845	0.875	0.905	1.139	1.179	1.229
78	0.846	0.876	0.906	1.136	1.176	1.225
80	0.848	0.878	0.907	1.134	1.173	1.222
85	0.852	0.881	0.91	1.129	1.166	1.213
90	0.855	0.883	0.912	1.124	1.16	1.206
95	0.858	0.886	0.914	1.12	1.155	1.199
100	0.861	0.888	0.916	1.116	1.15	1.192
110	0.866	0.893	0.92	1.11	1.141	1.181
120	0.871	0.897	0.923	1.104	1.133	1.171

Table 3: Auxiliary variables for the confidence interval for *m* (cont'd)

Statistical evaluation of σ_W (Maximum Likelihood confidence intervals)				
Input for statistical inference				
N	$b(N)$	$1-2\alpha$	$\alpha_1 = \alpha$	$\alpha_2 = 1-\alpha_1$

Maximum likelihood results	
$\widehat{\sigma_u}$	
$\hat{m}$	
$\hat{m}_{unb}$	

Auxiliary variables t_1, t_2, l_1, l_2	
$t_1(N, \alpha_1)$	
$t_2(N, \alpha_2)$	
$l_1(N, \alpha_1)$	
$l_2(N, \alpha_2)$	

Confidence limits		
	Lower limit A	Upper limit B
Confidence interval for σ_u:		
	Lower limit C	Upper limit D
Confidence interval for m:		

Table 4: Template for reporting Maximum Likelihood confidence intervals for Weibull stress calculations.

Statistical evaluation of σ_W (bootstrap confidence intervals)				
Input for statistical inference				
N	$b(N)$	$1-2\alpha$	$\alpha_1 = \alpha$	$\alpha_2 = 1-\alpha_1$

Maximum likelihood results	
$\widehat{\sigma_u}$	
$\hat{m}$	
$\hat{m}_{unb}$	

Auxiliary variables $z_0,\ z_0^m$	
z_0	
z_0^m	

Confidence limits		
	Lower limit A	Upper limit B
Confidence interval for σ_u:		
	Lower limit C	Upper limit D
Confidence interval for m:		

Table 5: Template for reporting bootstrap confidence intervals for Weibull stress calculations.